Journal of Polymers and the Environment (2022) 30:3078–3090
https://doi.org/10.1007/s10924-022-02398-1

ORIGINAL PAPER

Characterization of Physicochemical and Antibacterial Properties of Gelatin and Inulin Nanobiocomposite Films Containing Crystalline Nanocellulose and *Malva sylvestris* Extract

Haleh Dabbagh Nikoukheslat[1] · Ainaz Alizadeh[1] · Leila Roufegarinejad[1] · Shahram Hanifian[1]

Accepted: 1 February 2022 / Published online: 9 March 2022

Abstract
This study aimed to develop and characterize gelatin and inulin nanobiocomposite films with crystalline nanocellulose (CNC) and *Malva sylvestris* extract (MSE) for an active packaging system application. Fourier transform infrared structural conformations approved the formation of interactions between gelatin matrix, inulin, and other additives. According to the morphology study, the addition of inulin and CNC resulted in forming a dense and compact structure. Moreover, the addition of CNC enhanced the film samples' thermal properties and crystalline structure. The compensated for inulin's detrimental effect on mechanical parameters. The gelatin film sample containing CNC, MSE, and 50% inulin exhibited the least water vapor permeability, moisture content, and highest contact angle. The inclusion of CNC and inulin increased the L* value of the film samples significantly (p 0.05), which was reduced by incorporating MSE. Additionally, MSE-containing gelatin-based films inhibited *Listeria monocytogenes*, *Staphylococcus aureus*, and *Salmonella enteritis*. In conclusion, the combination of gelatin and inulin and the addition of CNC and MSE resulted in gelatin-based films with suitable physicochemical properties and antibacterial activity. Nanocomposite films developed in this study can be employed as an active packaging system for various foodstuffs.

Keywords Active packaging · Antibacterial activity · Nanofiller · Water barrier properties

Introduction

Food packaging is critical for preserving the quality of food products and preventing secondary contamination caused by chemicals, microorganisms, insects, rodents, and various environmental factors such as heat, humidity, light, and oxygen [1]. Nowadays, petroleum-based plastics are less popular due to their non-biodegradability and severe environmental risks associated with their pollution [2, 3]. To this end, developing biodegradable packaging with good mechanical and barrier properties represents a novel strategy for addressing the disadvantages of synthetic plastics [4, 5]. Biopolymers such as polysaccharides, proteins, lipids, and their composites serve as the base materials for biodegradable packaging [6, 7]. Thus, gelatin is a protein-based biopolymer that has garnered scientific interest for its biodegradability, low melting and gelling points, abundance, excellent film-forming ability, efficient oxygen barrier properties, and potential as a carrier for functional and antimicrobial agents [8, 9]. However, gelatin-based films exhibit poor mechanical and water barrier properties, limiting their application in food packaging. Gelatin can be combined with other nanoreinforcements and biopolymers, such as crystalline nanocellulose and inulin, to create composite films that overcome this limitation [10–12]. is a linear polysaccharide derived from plants that are considered a prebiotic. It confers health benefits on the host by lowering serum lipids, improving immune system function, increasing calcium absorption, and promoting regular bowel habits [13–15]. Furthermore, inulin's physicochemical properties, such as film-forming capacity, make it a more appealing biopolymer for use in the formulation of nanocomposite films [16]. In this regard, previous research has demonstrated that inulin has the potential to enhance the physical and structural properties of nanocomposite films composed of chitosan [14], carboxymethyl cellulose [17], gelatin [18], and cassava

✉ Ainaz Alizadeh
a.alizadeh@iaut.ac.ir

[1] Department of Food Science and Technology, Tabriz Branch, Islamic Azad University, Tabriz, Iran

starch [19]. Crystalline nanocellulose is a biodegradable, non-toxic compound with high mechanical strength and a demonstrated capacity for reinforcing polymers [20, 21]. These effects are related to the stiffness and strength of the CNCs, as well as a mechanical percolation effect caused by the CNCs' hydrogen bonding interactions and the formation of a continuous structure [22]. CNCs have also been shown to improve the barrier properties of a variety of film matrices, including alginate-acerola puree [23], hydroxypropyl methylcellulose (HPMC) [24], and chitosan [25], by forming long and tortuous (zigzag) pathways. When well-dispersed in the biopolymer matrix, nanofillers can also provide controlled release of active compounds such as antioxidants and antimicrobial agents [5]. The *Malva sylvestris* L. plant, also known as common *mallow*, is a member of the *Malvaceae* family and exhibits various therapeutic properties. Moreover, it is used as an antitussive, antiseptic, sedative, expectorant, bronchodilator, antidiarrheal, and is highly recommended for acne and skin care treatment [26]. MSE is a source of vitamin E, β-carotene, vitamin C, polyphenols, and other essential phytochemicals with extraordinary antioxidant and antimicrobial properties [27, 28]. MSE exhibits a potent antimicrobial effect against gram-negative and gram-positive bacteria, yeasts, and molds, according to previous literature [26, 29].

So far, a few studies were conducted to improve the functionality restrictions of the gelatin-based films using pullulan [12], montmorillonite [30], nano titanium dioxide [31], chitosan nanofiber, and ZnO nanoparticles [11]. However, to the best of our knowledge, no research has been conducted on the use of MSE as an antimicrobial and antioxidant agent as well as crystalline nanocellulose as a reinforcement agent in the formulation of gelatin and inulin-based biodegradable films. Thus, the purpose of this study was to prepare and characterize nanobiocomposite films composed of gelatin and inulin that were reinforced with CNC and activated with MSE extract.

Materials and Methods

Materials

Gelatin (medium molecular weight and purity of 99%) was obtained from Sigma-Aldrich Co. (St. Louis, USA). Inulin with a purity of 99.99% was purchased from Pars Abtin Tirajeh Co. (Tehran, Iran). Crystalline nanocellulose with a purity of =99% and particle size of 20-40 nm was purchased from the Nano Novin Polymer Co. (Gorgan, Iran). Glycerol (with the purity of 99.5% (W/W) was obtained from Merck Chemicals Co. (Darm-Stadt, Germany). *Malva sylvestris* extract was purchased from Adonis Gol Darou Co. (Tehran, Iran). Calcium sulfate, sodium chloride, potassium sulfate, and magnesium nitrate were procured from Merck Chemicals Co. (Darm-Stadt, Germany). *Listeria monocytogenes* (PTCC 1298), *Yersinia enterocolitica* (PTCC 1786), *Escherichia coli* (PTCC 1163), *Salmonella enterica* serovar Enteritidis (ATCC 13,076), *Staphylococcus aureus* (PTCC 1764), and *Pseudomonas aeruginosa* (PTCC 1310) were procured from Persian Type Culture Collection (PTCC) (Tehran, Iran). Mueller-Hinton agar for microbiological tests was procured from Sigma-Aldrich Co.(St.Louis, USA).

Preparation of Nanocomposite Film

The nanobiocomposite film samples were coded as Table 1. Briefly, the gelatin solution containing (5% w/v) gelatin and inulin, which replaced at different ratios (0, 25, and 50% w/v) based on gelatin weight was prepared through the dispersion of gelatin and inulin in distilled water and mixed for

Table 1 The fabricated gelatin-based nanobiocomposite film samples

Samples	Gelatin (% w/v)	Inulin (% w/v)	CNC (% w/v)	MSE (% v/v)
Control	100	0	0	0
G/MSE5%	100	0	0	5
G/CNC5%	100	0	5	0
G/CNC5%/MSE5%	100	0	5	5
G/IN25%	75	25	0	0
G/IN25%/MSE5%	75	25	0	5
G/IN25%/CNC5%	75	25	5	0
G/IN25%/CNC5%/MSE5%	75	25	5	5
G/IN50%	50	50	0	0
G/IN50%/MSE5%	50	50	0	5
G/IN50%/CNC5%	50	50	5	0
G/IN50%/CNC5%/MSE5%	50	50	5	5

G: gelatin, IN: inulin, CNC: crystallinenanocellulose, MSE: *Malva sylvestris* extract

30 min at 70 °C. Consequently, 0.8% glycerol (40% based on the dry matter) as a plasticizer and CNC were incorporated into the previously prepared solutions to reach a final concentration of (0 and 5% w/v) CNC based on gelatin-inulin weight and stirred for 30 min at 70 °C to reduce accumulation and uniform dispersion of nanoparticles. Then, the prepared film solutions were maintained at room temperature. *Malva sylvestris* extract in different concentrations (0 and 5% v/v) based on solution weight was added as an antimicrobial and antioxidant agent in the initial formulation and stirred for 5 min. Finally, the prepared film solutions were cast onto the polystyrene plates and dried at 40 °C for 48 h. The dried films were conditioned at RH=53% in a desiccator containing a saturated solution of $Mg(NO_3)_2$ for 72 h at 25 °C before further testing [9].

Fourier Transforms Infrared Spectroscopy (FTIR)

The FTIR spectra (Equinox 55LS 101, Bruker, Ettlingen, Germany) were used to analyze the structural interactions of gelatin-inulin films containing crystalline nanocellulose and *Malva sylvestris* extract. The FTIR spectra of gelatin-based films were recorded in the wavenumber range from 4000 to 500 cm^{-1} at resolutions of 8 cm^{-1}using the KBr^- pellet method.

Field Emission Scanning Electron Microscopy (FE-SEM)

The surface morphology of the films was examined by FE-SEM (Sigma VP, Zeiss, Obercochen, Germany). Samples were gold-coated using a direct current sputtering technique (DST1, nanostructured Coating, Tehran, Iran).

Differential Scanning Calorimetry (DSC)

The thermal properties of nanocomposite films were determined using differential scanning calorimetry (DSC6000 PerkinElmer, Waltham, MA, USA). 20 ± 5 mg of samples were heated at temperature ranges between 25 and 250 ℃ at a heating rate of 10 ℃/min under nitrogen atmosphere (20 ml/min) and were placed in a sample pan, and an empty pan was used as a reference. The glass transition temperature (Tg) of the samples were recorded.

X-ray Diffraction (XRD) Analyses

XRD patterns were used to study the crystalline structure of the nanocomposite films (Kristalloflex D500, Siemens, Munchen, Germany). Refractive radiation from the sample at room temperature and in the range of (2?) from 5° to 45° was recorded. The XRD analysis used the Cu Ka radiation source (k = 0.154 nm) operating at 40 kV and 40 mA.

Thickness Measurement

A digital micrometer (Fowler, Massachusetts, USA) with a precision of 0.01 mm was used to measure the thickness of the nanobiocomposite films. Ten measurements were taken from different parts of the films (center and perimeter) to ensure results consistency. The average thickness value was used to calculate mechanical and barrier properties.

Mechanical Properties

The standard method ASTM D882-95, used for the measurement of the ultimate tensile strength (UTS) and elongation at break (EB), was assessed with the Tensile Analyzer (INSTRON 5566, Massachusetts, USA). The films samples were cut into dumbbell shape (8 cm־ו.5 cm) and mounted into Initial grip separation, and cross-head speeds were set at 50 mm and 1 mm/min, respectively [5].

Water Vapor Permeability (WVP)

Gravimetrically methodology was used for the determination of the water vapor permeability (WVP) of films, employing an ameliorated ASTM E96-05 procedure (ASTM, 2005). The film samples (2?×2 cm) were sealed on glass vials containing dried anhydrous $CaSO_4$ to reach the vials inside RH to 0%. Each vial were placed at 25 °C in a desiccator containing K_2SO_4 solution to maintain the RH of 97% and the vials were weighed every 24 h using a digital balance (AND, Model HR 200, Tokyo, Japan). The weight changes of the vials (to the nearest 0.001 mg) have been recorded for 7 days. Consequently, the slope (changes of weight versus time) was calculated by linear regression. The water vapor transmission rate (WVTR) and water vapor permeability (WVP) of film samples were calculated as:

$$J = WVTR = \frac{\Delta W/\Delta t}{A}$$

$$WVP = \frac{WVTR \times X}{P(R_1 - R_2)}$$

where P is the saturation vapor pressure of water (P_a) at the test temperature (25 °C). R_1 is the RH in the desiccator, R_2 is the RH inside the vial, and X is the average thickness of film samples (m).

Moisture Absorption

Moisture absorption of film samples was assessed based on the method of Neus Angle`s and Dioufers [32]. Firstly, the films samples were cut into squares with dimensions 20 mm ɪ20 mm and placed inside a desiccator containing calcium sulfate (RH = 0%) for 24 h. After initial weighing, the samples were transferred to a desiccator containing sodium chloride saturated solution (RH = 75%) and stored at 20 to 25 °C. Then, all samples were weighed at desired time intervals until a constant weight was reached. Finally, the moisture absorption was calculated from the ratio of:

$$Moisture\ absorption(\%) = \frac{W_i - W_0}{W_0} \times 100$$

where, W_0 is the initial weight of the sample and W_t is the weight of the sample at 75% RH after t time.

Water Contact Angle

The surface wettability of films was evaluated from the contact angle measurements between films surface and water with a sessile drop method. After fixing the films to glass slides, a droplet of distilled water (5 µL) was placed over the surface of films using a syringe, and the images were captured with a camera (Canon MV50, Taiwan) at 0 and 60 s. Data were obtained by analyzing the image with Image J 1.48 software [33].

Color Measurement

Color parameters of nanobiocomposite films were measurement using a CIE colorimeter (Minolta CR300 158 Series, Minolta Camera Co. Ltd., Osaka, Japan). The color of the film samples was expressed as L* (lightness/brightness), a* (redness/greenness), and b* (yellowness/blueness) values. The film samples and RAL standard color sheets were placed in the standard box and imaged using a digital camera (Canon Power Shot SX720 HS, Japan). Then, the L*, a* and b* factors of film samples and RAL standard color sheets were shown by Adobe Photoshop software. After that, the calibration curves were found by drawing the actual L*, a*, and b* values of the standard sheets against the showed values by software. The L*, a*, and b* values of film samples were measured using software's replacement of showed factors in the equations of calibration curves [9].

Antibacterial Activity

The agar disc diffusion method was used to determine the antibacterial activity of the nanobiocomposite film samples against six foodborne pathogenic bacteria, *Listeria monocytogenes*, *Staphylococcus aureus*, *Escherichia coli*, *Salmonella enterica* serovar Enteritidis, *Yersinia enterocolitica*, *Pseudomonas aeruginosa*. The suspensions containing 1.5?×0^8 CFU/mL bacteria were prepared and cultured on the prepared Mueller Hinton Agar plate surface. The film sample was cut to a round disc with a 7 mm diameter and was put on the surface of Mueller Hinton agar plates. After incubation at 37 °C for 24 h, the diameter of the inhibition zone around the film sample was determined in triplicate by the caliper and the means were reported [7].

Statistical Analysis

Statistical analysis was performed based on one-way analysis of variance (ANOVA) using IBM SPSS Statistics 22 (IBM Corporation, Armonk, NY, USA). Duncan's multiple test range (p ? 0.05) was used to detect significant differences among values. Data presented as means of three replications ± standard deviations.

Results and Discussion

Chemical and Microstructural Characterization of the Nanobiocomposite Films

The FT-IR spectra of film samples are depicted in Fig. 1. The neat gelatin film's spectrum revealed several distinct peaks at 3437, 2961, 1641, 1544, and 1054 cm^{-1}. The broad and strong band at 3437 cm^{-1} was attributed to N–H stretching

and hydrogen bonding in the amide-A band [34]. The band at 2961 cm^{-1} was associated with the symmetry C–H stretching mode [12]. The peaks at 1641 and 1544 cm^{-1} were determined to be associated with the C=O and C-N stretching vibrations of amide I and II, respectively [35, 36]. The peak at 1054 cm^{-1} indicated the interaction of glycerol's OH group with gelatin [17]. According to the results, the changes in the spectra of neat gelatin film by incorporating CNC and inulin could be the result of the conformation of gelatin polypeptide chains, which decreased the presence of single a-helices, random coils, and disordered structures. In this regard, MSE, CNC, and inulin incorporation into gelatin-based films resulted in the following spectral changes: (1) the peak at 3437 cm^{-1} shifted to higher wavenumbers, and (2) the peak at 1544 cm^{-1} shifted to lower wavenumbers. Thus, the G/IN50%/CNC5%/MSE5% film sample spectrum revealed distinct peaks at 3447, 2952, 1646, 1519, and 1046 cm^{-1}. The spectral changes caused by the addition of MSE, CNC, and inulin to gelatin-based films can be explained by the conversion of gelatin's functional groups and the formation of interactions (hydrogen bonds) between the gelatin matrix and additives. Similar findings have been reported previously for incorporated gelatin-based films with CNC [36, 37] and cellulose nanofiber [38]. In a similar study, it was observed that the intensity of the band at 1030 cm^{-1} increased for gelatin nanobiocomposites with 10 wt% CNCs and 10 wt% CNF [39]. Zabihollahi et al. [17] reported that a slight change was observed in the bands related to the hydroxyl and carboxylate groups by incorporation of CNF and inulin that can be attributed to possible interactions (hydrogen bonds) between CNF and inulin. The primary spectral changes caused by the incorporation of these nanoparticles were observed in the bands of hydroxyl, amino, and amide groups, which is consistent with our findings.

Figure 1.

Morphological Characterization of the Nanobiocomposite Films

The surface and cross-section FE-SEM images of the gelatin-based nanobiocomposite film are displayed in Fig. 2. As can be seen, the neat gelatin film had a homogeneous and compact morphology devoid of pores (Fig. 2 A and 2a). However, few cracks were observed in the G/MSE5% sample's surface and cross-section microstructures (Fig. 2B and b). While incorporating CNC into the gelatin-based film resulted in a denser surface image (Fig. 2 C), a few cracks were observed in the cross-section microstructure (Fig. 2c). As illustrated in Fig. 2D and d, the addition of 50% inulin resulted in a more compact and dense structure. However, some small agglomerates were observed in the G/IN50% film sample's surface and cross-section microstructures. These agglomerations may be related to inulin accumulation at a high concentration in the polymer matrix. According to the results, the microstructures of the G/IN50%/CNC5%/MSE5% film sample (Fig. 2E and e) were the most compact and dense of all samples. Additionally, inulin accumulations were lower in this sample, particularly in the cross-section microstructure, than in the G/IN50% sample. This effect of CNC and inulin on filling structural void spaces and the formation of strong interactions between the gelatin matrix and additives can be attributed to the formation of a more compact structure [34]. Similarly, gelatin-based film samples containing cellulose nanocrystals [36], copper nanoclusters [40], and cellulose nanofibers [38, 41] have been reported to exhibit similar properties. Leite et al. (2020) reported that the neat gelatin film displayed a continuous and homogeneous matrix with a smooth fractured surface and the addition of CNCs gradually promoted the formation of a rougher fractured surface, indicating a microstructural change in the gelatin matrix. However, no clear evidences of CNCs agglomerates were detected in all the bionanocomposite micrographs, suggesting that the CNCs were homogeneously distributed within the gelatin matrix.

Thermal Stability of the Nanobiocomposite Films

The DSC analysis determined the thermal properties of film samples, and the resulting DSC thermograms are shown in Fig. 3a. The control film sample's glass transition temperature (T_g) was 30.0 °C. Our findings corroborated with Fakhreddin Hosseini et al. [42], who reported that the T_g of the neat gelatin film was 29.8 °C. According to the results, the addition of MSE had no discernible effect on the T_g. The addition of 50% inulin, on the other hand, resulted in a decrease in the T_g value of the film samples to 26.0 °C. This decrease was offset by the addition of CNC, which resulted in an increase in the T_g value of the G/IN50%/CNF5%/MSE5% film sample to 29.6 °C. Similar findings have been observed when inulin and cellulose nanofibers were added to carboxymethyl cellulose-based films [17]. T_g represents the miscibility of materials; at temperatures above it, the structure of amorphous materials changes from a glassy to a viscous state [43]. Thus, the increase in T_g caused by CNC incorporation can be attributed to the decreased mobility of gelatin chains caused by the formation of interactions

Table 2 The thickness and mechanical properties of nanobiocomposite film samples

Film samples	Thickness (mm)	UTS (MPa)	EB (%)
Control	0.23 ± 0.04^{a}	4.03 ± 1.25^{a}	145.84 ± 23.46^{e}
G/MSE5%	0.19 ± 0.03^{c}	3.41 ± 0.23^{ab}	155.02 ± 1.18^{de}
G/CNC5%	0.21 ± 0.04^{b}	3.26 ± 0.68^{ab}	166.38 ± 31.86^{cde}
G/CNC5%/MSE5%	0.19 ± 0.05^{c}	3.17 ± 1.08^{abc}	162.97 ± 38.43^{de}
G/IN25%	0.20 ± 0.04^{bc}	3.39 ± 1.16^{ab}	214.24 ± 62.42^{bcd}
G/IN25%/MSE5%	0.20 ± 0.05^{bc}	2.73 ± 0.21^{bcd}	215.10 ± 28.34^{bcd}
G/IN25%/CNC5%	0.19 ± 0.04^{c}	3.21 ± 0.66^{abc}	215.71 ± 35.46^{bcd}
G/IN25%/CNC5%/MSE5%	0.19 ± 0.05^{c}	2.12 ± 0.36^{bcd}	166.98 ± 32.70^{cde}
G/IN50%	0.20 ± 0.04^{bc}	2.19 ± 0.09^{bcd}	262.04 ± 18.90^{ab}
G/IN50%/MSE5%	0.20 ± 0.05^{bc}	1.77 ± 0.19^{d}	228.17 ± 10.74^{bc}
G/IN50%/CNC5%	0.20 ± 0.05^{bc}	2.16 ± 0.22^{bcd}	318.58 ± 16.55^{a}
G/IN50%/CNC5%/MSE5%	0.20 ± 0.03^{bc}	1.94 ± 0.29^{cd}	241.02 ± 52.81^{b}

Data are expressed as mean ± standard deviation (n = 3) and different letters in the same column show significant difference at the 5% level in Duncan's test ($p < 0.05$) *UTS* ultimate tensile strength, *EB* elongation at break, *G* gelatin, *IN* inulin, *CNC* crystallinenanocellulose, *MSE Malva sylvestris* extract

between the CNC and the gelatin matrix. Previously published research indicated that incorporating CNC and cellulose nanofibers into fish myofibrillar protein [44] and gelatin [45] films enhanced their thermal properties by forming a compact matrix with high thermal stability.

Crystallinity Structure of the Nanobiocomposite Films

The XRD diffractograms of the gelatin-based nanobiocomposite film samples are shown in Fig. 3b. Two distinct peaks at 2? of 13.45° and 20.10° were observed in the XRD pattern of the neat gelatin film, which corresponded to the gelatin's a-helix and β-sheet structures. Earlier studies [38, 46] reported comparable results for XRD analyses of the neat gelatin film. The diffractogram of the MSE-incorporated film revealed three distinct peaks at 2? of 30°, 20.47°, and 30.97°, indicating that the crystalline structure has changed due to MSE incorporation. CNC enhanced this change in the crystalline structure, and the G/CNF5% exhibited peaks at 2? of 12.80°, 20.30°, 22.91º, and 30.94º. Moreover, the G/IN50% showed three distinct peaks at 2? of 12.48°, 21.50°, and 30.98°. Thus, incorporating all additives, namely MSE, CNC, and inulin, in gelatin-based films resulted in a change in peak positions, with CNC causing the most significant change. These findings are consistent with the high crystalline structure of CNC, which resulted in an increase in the crystallinity index and rigidity of gelatin-based films. In line with our findings, Li et al. (2017) reported that the XRD pattern of the soy protein isolate film incorporated with microcrystalline cellulose exhibited relatively high peaks indicative of microcrystalline cellulose's high crystalline structure. As illustrated in Fig. 3b, three distinct peaks were observed at 2? of 12.81°, 21.22°, and 30.95° in the diffractogram of G/IN50%/CNF5%/MSE50%. Generally, the obtained results indicated that incorporating all three additives that represent the compatibility film matrix and additives improved the crystallinity in gelatin-based films.

Thickness and Mechanical Properties

The thickness and mechanical properties of the film samples are listed in Table 2. As a result of the incorporation of MSE, CNC, and inulin at various concentrations, the thickness values of the gelatin-based films were significantly ($p < 0.05$) decreased. Additionally, there was no significant difference in the thickness values of the combined film samples containing MSE, CNC, and inulin ($p > 0.05$). The thickness of film samples ranged between 19 and 23 mm. In line with our results, Zabihollahi et al. [17] reported that

Table 3 The water barrier properties of nanobiocomposite film samples

Film samples	WVP (•0^{-7} g/m.s.Pa)	Moisture absorption (%)	Water contact angle (°)
Control	6.80 ± 0.36^{a}	22.98 ± 0.32^{a}	33.75 ± 0.73^{f}
G/MSE5%	5.36 ± 0.11^{d}	22.18 ± 1.29^{ab}	34.11 ± 0.95^{f}
G/CNC5%	6.10 ± 0.30^{abc}	21.70 ± 1.41^{ab}	38.31 ± 0.65^{de}
G/CNC5%/MSE5%	5.16 ± 0.32^{d}	20.69 ± 1.01^{b}	40.13 ± 2.40^{bcd}
G/IN25%	6.40 ± 0.60^{ab}	21.65 ± 0.42^{ab}	41.89 ± 0.95^{ab}
G/IN25%/MSE5%	6.60 ± 0.60^{a}	21.26 ± 0.21^{b}	38.97 ± 1.50^{cde}
G/IN25%/CNC5%	6.10 ± 1.08^{abc}	21.76 ± 1.07^{b}	40.25 ± 0.79^{bcd}
G/IN25%/CNC5%/MSE5%	6.40 ± 0.20^{ab}	20.77 ± 0.90^{b}	40.88 ± 1.53^{bc}
G/IN50%	6.26 ± 0.11^{ab}	18.47 ± 0.83^{cd}	39.92 ± 1.03^{bcd}
G/IN50%/MSE5%	5.80 ± 0.20^{bcd}	17.80 ± 0.02^{d}	40.06 ± 0.58^{bcd}
G/IN50%/CNC5%	6.60 ± 1.08^{a}	19.29 ± 0.45^{c}	37.38 ± 0.57^{e}
G/IN50%/CNC5%/MSE5%	5.40 ± 0.80^{cd}	17.75 ± 0.16^{d}	43.15 ± 0.55^{a}

Data are expressed as mean ± standard deviation (n = 3) and different letters in the same column show significant difference at the 5% level in Duncan's test ($p < 0.05$). *WVP* water vapor permeability, *G* gelatin, *IN* inulin, *CNC* crystallinenano cellulose, *MSE Malva sylvestris* extract

incorporating cellulose nanofibers into carboxymethyl cellulose films resulted in a reduction trend in the thickness values.

The UTS and EB parameters of neat gelatin film were 4.03 ± 1.25 MPa and 145.84 ± 23.46%, respectively, as shown in Table 2. The addition of MSE and CNC had no significant effect on the UTS values of gelatin-based films ($p > 0.05$). Although there was no significant difference in the UTS values of film samples containing 25% inulin, the films' UTS values were significantly decreased when the inulin concentration was increased to 50%. Among the combined samples containing MSE, CNC, and inulin, the G/IN25%/CNC5% film sample had the highest UTS value (3.21 ± 0.66 MPa). However, no significant difference in UTS values was observed between G/IN25%/CNC5%/MSE5% and G/IN50%/CNC5%/MSE5% films. Individual additions of MSE and CNC had no discernible effect on the EB values of gelatin-based films. However, supplementation with inulin has been shown to increase EB values significantly. As a result, the highest value of EB in the combined film samples was associated with the G/IN50%/CNC5% (318.58 ± 16.55%). Moreover, it should be noted that the EB value of the G/IN25%/CNC5%/MSE5% sample did not differ significantly from the control sample. Generally, the negative effect of inulin on mechanical parameters was compensated for by incorporating CNC, which owes its strength and rigidity to its natural properties and the formation of additional interactions in the film matrix [17]. In this regard, it has been reported that the mechanical properties of a film matrix are significantly influenced by the inter-and intramolecular interactions between the polymer chains [34]. Previously published research indicated that adding CNC to gelatin-based films increased the UTS and EB values via the formation of hydrogen bonds between the hydrophilic amino acids in the gelatin chains and the CNC hydroxyl groups, thereby strengthening the gelatin-CNC interface [36, 37]. The UTS and EB values remained constant after incorporating CNC in our study due to the low concentration of the incorporated CNC. Similar results have been reported when cellulose nanofiber and inulin were incorporated into carboxymethyl cellulose films [17].

Water Barrier Properties

Water vapor permeability (WVP), moisture absorption, and water contact angle were used to determine the film samples' water barrier properties. As shown in Table 3, the neat gelatin film had a WVP value of 6.80 ± 0.36?×10^{-7} g/m.s.Pa. The WVP values of the films did not change significantly ($p > 0.05$) when CNC and inulin were added separately. The addition of MSE, on the other hand, significantly decreased the WVP value to 5.36 ± 0.11?×10^{-7} g/m.s.Pa. Among

Table 4 Color parameters of nanobiocomposite film samples

Film sample	L*	a*	b*
Control	71.75 ± 0.66^{b}	-14.10 ± 8.59^{b}	21.58 ± 5.62^{c}
G/MSE5%	65.60 ± 0.80^{cd}	-21.40 ± 1.24^{b}	39.33 ± 0.57^{a}
G/CNC5%	73.60 ± 0.34^{a}	-6.33 ± 2.28^{a}	19.00 ± 0.91^{cd}
G/CNC5%/MSE5%	67.03 ± 0.72^{c}	-21.66 ± 0.30^{b}	37.73 ± 0.98^{ab}
G/IN25%	74.06 ± 0.30^{a}	-6.66 ± 2.57^{a}	18.33 ± 0.30^{cd}
G/IN25%/MSE5%	64.96 ± 0.56^{d}	-21.93 ± 0.11^{b}	37.46 ± 1.27^{ab}
G/IN25%/CNC5%	74.36 ± 0.70^{a}	-19.78 ± 0.20^{b}	18.46 ± 0.50^{cd}
G/IN25%/CNC5%/MSE5%	61.53 ± 2.36^{e}	-21.53 ± 0.46^{b}	36.60 ± 0.87^{ab}
G/IN50%	74.80 ± 1.21^{a}	-14.73 ± 9.12^{b}	13.13 ± 8.42^{d}
G/IN50%/MSE5%	62.53 ± 0.90^{e}	-17.66 ± 7.50^{b}	31.73 ± 7.14^{b}
G/IN50%/CNC5%	73.93 ± 0.11^{a}	-20.33 ± 0.11^{b}	18.06 ± 0.11^{cd}
G/IN50%/CNC5%/MSE5%	62.91 ± 1.80^{e}	-6.95 ± 2.89^{a}	36.73 ± 0.94^{ab}

Data are expressed as mean ± standard deviation (n = 3) and different letters in the same column show significant difference at the 5% level in Duncan's test ($p < 0.05$). *G* gelatin, *IN* inulin, *CNC* crystallinenanocellulose, *MSE Malva sylvestris* extract

Table 5 The antimicrobial activity of nanobiocomposite film samples

Samples	Inhibitory zone (mm)					
	L. monocytogenesis	*S. aureus*	*E. coli*	*S. enterica*	*Y. enterocolitica*	*P. aeruginosa*
Control	10.13 ± 1.01^{d}	–	–	–	–	–
G/MSE5%	13.57 ± 0.92^{c}	16.27 ± 0.88^{c}	–	6.23 ± 0.61^{ns}	–	–
G/CNC5%/MSE5%	13.27 ± 0.52^{c}	15.86 ± 0.35^{c}	–	6.77 ± 0.48^{ns}	–	–
G/IN50%/MSE5%	15.85 ± 0.28^{b}	20.74 ± 1.25^{a}	–	6.97 ± 0.72^{ns}	–	–

Data are expressed as mean ± standard deviation (n = 3) and different letters in the same column show significant difference at the 5% level in Duncan's test ($p < 0.05$). *ns* no significant, *G* gelatin, *IN* inulin, *CNC* crystallinenanocellulose, *MSE Malva sylvestris* extract

the combined film samples, the G/CNC5%/MSE5%, G/IN50%/MSE5%, and G/IN50%/CNC5%/MSE5% samples demonstrated lower WVP values than the control sample. Individual additions of MSE and CNC had no discernible effect on the films' moisture absorption. Although there was no significant change in the moisture absorption of films containing 25% inulin, this value increased when the inulin loading concentration was increased to 50%. However, the lowest moisture absorption value (17.75 ± 0.16%) was associated with the G/IN50%/CNC5%/MSE5% sample, which demonstrated a significantly ($p < 0.05$) decreasing trend when MSE, CNC, and inulin were combined. The water contact angle is another critical parameter for determining the hydrophobicity of the surface [47].

As shown in Table 3, the addition of CNC and inulin increased the water contact angle values significantly, whereas the addition of MSE had no significant effect on the water contact angle. According to the results, the G/IN50%/CNC5%/MSE5% had the greatest water contact angle (43.15° ± 0.55°). In general, the obtained results indicated that CNC, inulin, and MSE have a beneficial effect on the water barrier properties of gelatin-based films, which is consistent with previous research [47]. CNC nanofillers are distributed throughout the film matrix, creating a tortuous path for water molecules to traverse [34]. Moreover, the incorporation of CNC and inulin results in filling open spaces between polymer chains and forming a compact structure, which increases resistance to water molecule penetration [17, 48]. Furthermore, the formation of hydrogen bonds between the gelatin matrix and the incorporated compounds reduced the gelatin structure's free hydrophilic groups [38]. As a result, these phenomena can be attributed to the enhancement of water barrier properties by CNC, inulin, and MSE. Similar findings have been reported previously to incorporate bacterial cellulose nanocrystals and cellulose nanofibers into gelatin-based films [37] and cellulose nanofiber [34]. Along with the previously mentioned mechanisms, Shabanpour et al. (2018) reported that the high crystallization level of cellulose nanofiber might be another compelling reason for its beneficial effect on the hydrophobicity of fish gelatin-based films.

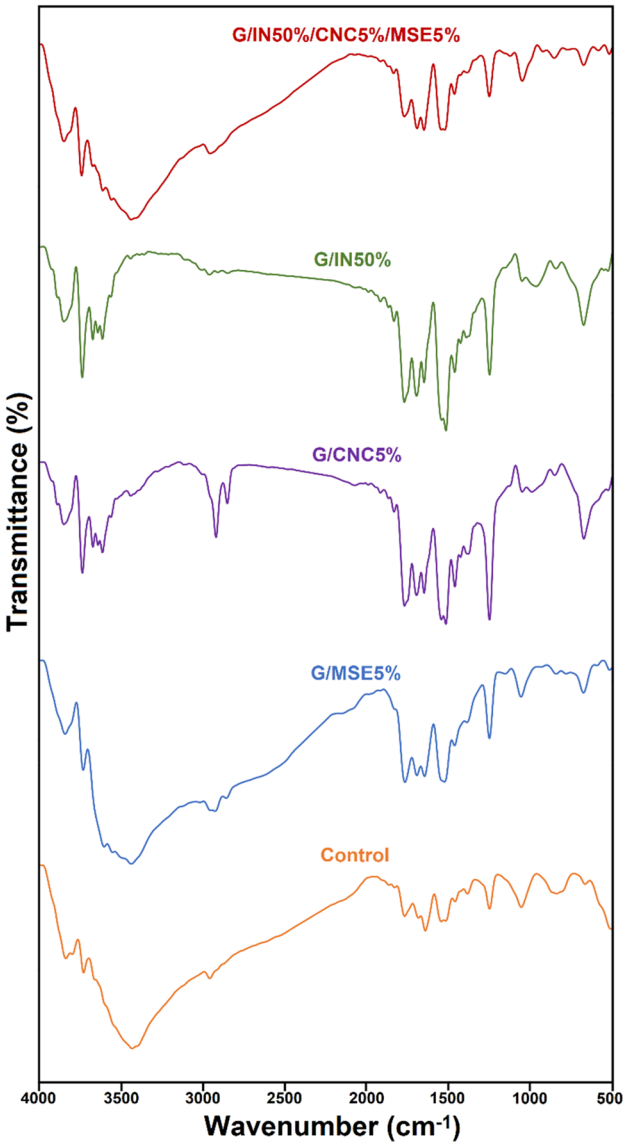

Fig. 1 FT-IR spectra of control, G/MSE5%, G/CNC5%, G/IN50%, and G/IN50%/CNC5%/MSE5% film samples. G: gelatin, IN: inulin, CNC: crystallinenanocellulose, MSE: *Malva sylvestris* extract

Color Measurement

The color properties of packaging systems have a significant impact on the overall appearance and acceptance of the product. Table 4 summarizes the color parameters of the film samples. As a result of the incorporation of MSE, the L* parameter of gelatin-based films decreased. Thus, all samples that contained MSE had a lower L* value than the control sample. However, when CNC and inulin were added to film samples, the L* parameter increased. The film samples incorporated with CNC or inulin and free of MSE had the highest values of the L* parameter. In contrast to our findings, it has been reported that incorporating cellulose nanofibers into fish myofibrillar protein films [44] and inulin into gelatin films [49] did not result in a significant change in the L* parameter of the film samples. Additionally, no significant difference in the a* parameter of film samples was observed when MSE was included. Individual incorporation of CNC and addition of inulin at a 25% concentration increased the a* values significantly ($p < 0.05$). Tibolla et al. [50] confirmed our findings by reporting that adding cellulose nanofibers to banana starch-based films increased their redness. However, except for the G/IN50%/CNC5%/MSE5% sample, the a* parameter of the films incorporating both or all three of MSE, CNC, and inulin showed no significant difference when compared to the control sample. This phenomenon indicated that when CNC and inulin were combined, their effects on the a* parameter were diminished.

As shown in Table 4, when MSE was included, the b* color parameter of film samples increased but was decreased by adding inulin at a 50% concentration. CNC and inulin at a concentration of 25% had no significant effect on the b* values ($p > 0.05$). All samples containing MSE had the highest b* color parameter values, which could be attributed to its chemical composition and natural yellow color, which increased the yellowness of film samples.

Antimicrobial Properties of the Nanobiocomposie Films

Table 5 shows the inhibition zone diameters of the film samples against six foodborne pathogenic bacteria. As a result, the neat gelatin film exhibited an inhibition zone for *L. monocytogenes* (10.13 ± 1.01 mm) but no inhibition for other bacteria. MSE incorporation increased the inhibitory activity against *L. monocytogenes* and provided inhibitory activity against *S. aureus* and *S. enteritidis* bacteria. MSE's antibacterial activity results from Malvone A, a phytoalexin and phenolic compound contained in this extract [51].

The G/IN50%/MSE5% sample exhibited the highest inhibition zones against *L. monocytogenes* (15.85 ± 0.28 mm) and *S. aureus* (20.74 ± 1.25 mm) bacteria but exhibited no inhibition activity against *E. coli*, *Y. enterocolitica*, and *P. aeruginosa* bacteria. However, no statistically significant difference in the inhibition activity of the film samples against *S. enteritidis* was observed. These findings indicated that the inhibitory activity of film samples against Gram-positive bacteria was more significant than their inhibitory activity against Gram-negative bacteria, which is consistent with previous research [52, 53]. This phenomenon is explained by differences in the structure of the bacterial membranes. Gram-positive bacteria have a thick cell wall composed of multiple layers of peptidoglycan. On the other hand, Gram-negative bacteria have a more sophisticated cell wall structure that includes a thin peptidoglycan layer and a barrier-like outer membrane. As a result, the outer membrane of Gram-negative

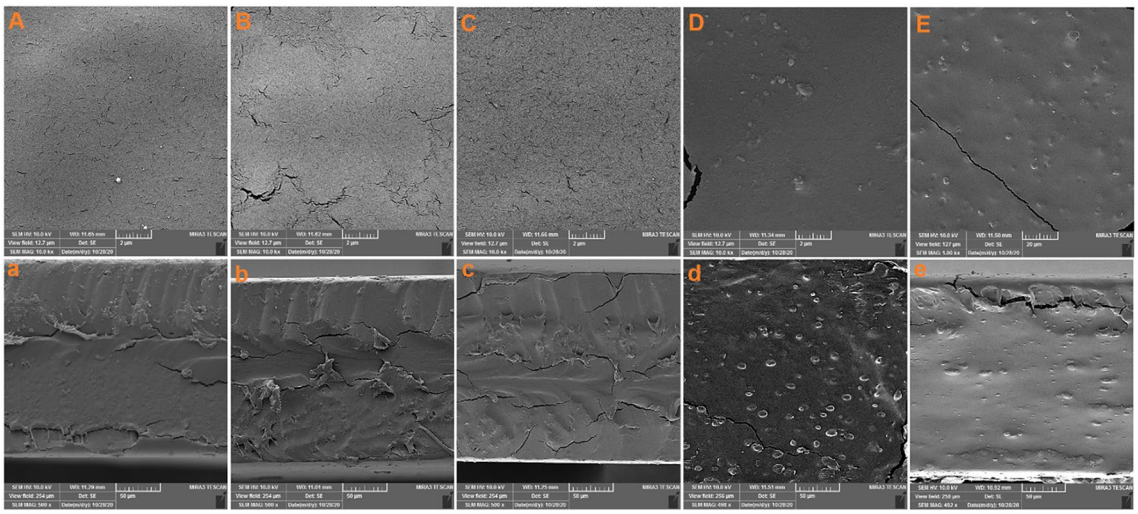

Fig. 2 Field emission scanning electron microscopy (FE-SEM) images of the surface and cross section of control (**A** and **a**), G/MSE5% (**B** and **b**), G/CNC5% (**C** and **c**), G/IN50% (**D** and **d**), and G/IN50%/CNC5%/MSE5% (**E** and **e**) film samples. G: gelatin, IN: inulin, CNC: crystallinenanocellulose, MSE: *Malva sylvestris* extract

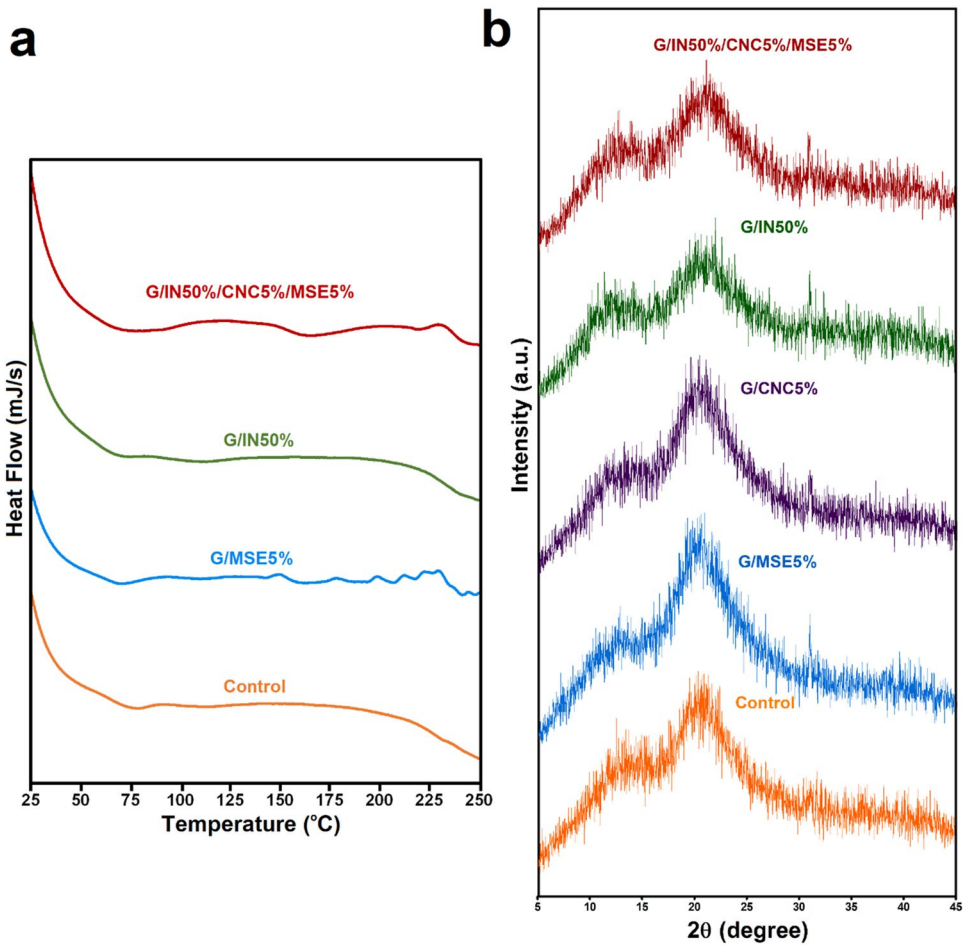

Fig. 3 The differential scanning calorimetry (DSC) thermograms (**a**) and the X-ray diffraction (XRD) patterns (**b**) of control, G/MSE5%, G/CNC5%, G/IN50%, and G/IN50%/CNC5%/MSE5% film samples. G: gelatin, IN: inulin, CNC: crystallinenanocellulose, MSE: *Malva sylvestris* extract

bacteria prevents antibacterial agents from penetrating the bacterial cell [54, 55].

Conclusions

CNC and MSE were successfully incorporated into films made of gelatin and inulin. The results of FT-IR, DSC, and XRD analysis confirmed the formation of interactions between gelatin matrix, inulin, CNC, and MSE, as well as their compatibility. SEM analysis revealed that the addition of inulin and CNF resulted in a dense and compact structure. G/IN50%/CNC5%/MSE5% exhibited the highest water barrier parameters and the most suitable mechanical properties. Additionally, the addition of MSE inhibited the growth of foodborne pathogenic bacteria in the gelatin-based films. Considering these results, incorporating CNC and inulin at a 50% concentration appears to be a promising method for enhancing the physicochemical properties of gelatin-based films. Moreover, as an active packaging system, the developed nanocomposite film could aid in extending the shelf life of food products.

Acknowledgements The authors gratefully thank the supports of the Islamic Azad University, Tabriz Branch, Tabriz, Iran. This research did not receive any specific grant from funding agencies in the public, commercial, or not-for-profit sectors.

Declarations

Conflict of interest The authors confirm that they have no conflicts of interest with respect to the work described in this manuscript.

References

1. Hernoaez-Cortez C, Palma-Martinez I, Gonzalez-Avila LU et al (2017) Food poisoning caused by bacteria (food toxins). Poison Specif Toxic Agents to Nov Rapid Simpl Tech Anal 33:1
2. Sherafatkhah Azari S, Alizadeh A, Asefi N, Hamishehkar H (2021) Investigation the effect of ZnO and β-glucan on chemical and microbial characteristic of gelatin based biodegradable film over storage of chicken fillet. Food Sci Technol 18:169–180
3. Mousavi Kalajahi SE, Alizadeh A, Hamishehkar H et al (2021) Orange juice processing waste as a biopolymer base for biodegradable film formation reinforced with cellulose nanofiber and activated with nettle essential oil. J Polym Environ. https://doi.org/10.1007/s10924-021-02195-2
4. Noorbakhsh-Soltani SM, Zerafat MM, Sabbaghi S (2018) A comparative study of gelatin and starch-based nano-composite films modified by nano-cellulose and chitosan for food packaging applications. Carbohydr Polym 189:48–55
5. Soofi M, Alizadeh A, Hamishehkar H et al (2021) Preparation of nanobiocomposite film based on lemon waste containing cellulose nanofiber and savory essential oil: A new biodegradable active packaging system. Int J Biol Macromol 169:352–361. https://doi.org/10.1016/j.ijbiomac.2020.12.114
6. Pereda M, Ponce AG, Marcovich NE et al (2011) Chitosan-gelatin composites and bi-layer films with potential antimicrobial activity. Food Hydrocoll 25:1372–1381
7. Karimi N, Alizadeh A, Almasi H, Hanifian S (2020) Preparation and characterization of whey protein isolate/polydextrose-based nanocomposite film incorporated with cellulose nanofiber and *L. plantarum*: a new probiotic active packaging system. LWT. https://doi.org/10.1016/j.lwt.2019.108978
8. Sahraee S, Milani JM, Ghanbarzadeh B, Hamishehkar H (2017) Physicochemical and antifungal properties of bio-nanocomposite film based on gelatin-chitin nanoparticles. Int J Biol Macromol 97:373–381
9. Amjadi S, Emaminia S, Nazari M et al (2019) Application of reinforced ZnO nanoparticle-incorporated gelatin bionanocomposite film with chitosan nanofiber for packaging of chicken fillet and cheese as food models. Food Bioprocess Technol 12:1205–1219. https://doi.org/10.1007/s11947-019-02286-y
10. Ramos M, Valdes A, Beltran A, GarrigC (2016) Gelatin-based films and coatings for food packaging applications. Coatings 6:41
11. Amjadi S, Emaminia S, Heyat Davudian S et al (2019) Preparation and characterization of gelatin-based nanocomposite containing chitosan nanofiber and ZnO nanoparticles. Carbohydr Polym 216:376–384. https://doi.org/10.1016/j.carbpol.2019.03.062
12. Shen Y, Ni ZJ, Thakur K et al (2021) Preparation and characterization of clove essential oil loaded nanoemulsion and pickering emulsion activated pullulan-gelatin based edible film. Int J Biol Macromol 181:528–539. https://doi.org/10.1016/j.ijbiomac.2021.03.133
13. Huebner J, Wehling RL, Parkhurst A, Hutkins RW (2008) Effect of processing conditions on the prebiotic activity of commercial prebiotics. Int Dairy J 18:287–293
14. Cao TL, Yang SY, Song K, Bin (2018) Development of burdock root inulin/chitosan blend films containing oregano and thyme essential oils. Int J Mol Sci 19:1–12. https://doi.org/10.3390/ijms19010131
15. Alizadeh A, Aghayi N, Soofi M, Roufegarinejad L (2021) Development of synbiotic added sucrose-free mango nectar as a potential substrate for Lactobacillus casei: Physicochemical characterisation and consumer acceptability during storage. Acta Aliment 50:299–309
16. Akhgari A, Farahmand F, Garekani HA et al (2006) Permeability and swelling studies on free films containing inulin in combination with different polymethacrylates aimed for colonic drug delivery. Eur J Pharm Sci 28:307–314
17. Zabihollahi N, Alizadeh A, Almasi H et al (2020) Development and characterization of carboxymethyl cellulose based probiotic nanocomposite film containing cellulose nanofiber and inulin for chicken fillet shelf life extension. Int J Biol Macromol 160:409
18. Temiz NN, demir KS (2021) Microbiological and physicochemical quality of strawberries (Fragaria ananassa) coated with *Lactobacillus rhamnosus* and inulin enriched gelatin films. Postharvest Biol Technol. https://doi.org/10.1016/j.postharvbio.2020.111433
19. Orozco-Parra J, MejM, Villa CC (2020) Development of a bioactive synbiotic edible film based on cassava starch, inulin, and *Lactobacillus casei*. Food Hydrocoll. https://doi.org/10.1016/j.foodhyd.2020.105754
20. Chaichi M, Hashemi M, Badii F, Mohammadi A (2017) Preparation and characterization of a novel bionanocomposite edible film based on pectin and crystalline nanocellulose. Carbohydr Polym 157:167–175. https://doi.org/10.1016/j.carbpol.2016.09.062
21. Huq T, Fraschini C, Khan A et al (2017) Alginate based nanocomposite for microencapsulation of probiotic: Effect of cellulose

nanocrystal (CNC) and lecithin. Carbohydr Polym 168:61–69. https://doi.org/10.1016/j.carbpol.2017.03.032
22. Azeredo HMC, Rosa MF, Mattoso LHC (2017) Nanocellulose in bio-based food packaging applications. Ind Crops Prod 97:664–671. https://doi.org/10.1016/j.indcrop.2016.03.013
23. Azeredo HMC, Miranda KWE, Rosa MF et al (2012) Edible films from alginate-acerola puree reinforced with cellulose whiskers. LWT-Food Sci Technol 46:294–297
24. George J, Kumar R, Sajeevkumar VA et al (2014) Hybrid HPMC nanocomposites containing bacterial cellulose nanocrystals and silver nanoparticles. Carbohydr Polym 105:285–292
25. Khan A, Khan RA, Salmieri S et al (2012) Mechanical and barrier properties of nanocrystalline cellulose reinforced chitosan based nanocomposite films. Carbohydr Polym 90:1601–1608
26. Alexieva IN, Baeva MR, Popova AT et al (2021) Edible coatings enriched with *Malva sylvestris* L. extract. IOP Conf Ser Mater Sci Eng. https://doi.org/10.1088/1757-899X/1031/1/012113
27. Tabaraki R, Ali Asadi Gharneh H (2012) Chemical Composition and Antioxidant Properties of Malva Sylvestris L. urnal Res Agric Sci 8:59–68
28. Samavati V, Manoochehrizade A (2013) Polysaccharide extraction from Malva sylvestris and its anti-oxidant activity. Int J Biol Macromol 60:427–436
29. Cecotti R, Bergomi P, Carpana E, Tava A (2016) Chemical characterization of the volatiles of leaves and flowers from cultivated malva sylvestris var. mauritiana and their antimicrobial activity against the aetiological agents of the european and American foulbrood of honeybees (apis mellifera). Nat Prod Commun 11:1527–1530. https://doi.org/10.1177/1934578x1601101026
30. Echegaray M, Mondragon G, Martin L et al (2016) Physicochemical and mechanical properties of gelatin reinforced with nanocellulose and montmorillonite. J Renew Mater 4:206–214. https://doi.org/10.7569/JRM.2016.634106
31. Nassiri R, Mohammady Nafchi A (2013) Antimicrobial and barrier properties of bovine gelatin films reinforced by nano TiO2. J Chem Heal Risks 3:21–28
32. Neus Angles M, Dufresne A (2000) Plasticized starch/tuniein whiskers nanocomposites. 1. Structural analysis. Macromolecules 33:8344–8353. https://doi.org/10.1021/ma0008701
33. Fathi N, Almasi H, Pirouzifard MK (2018) Effect of ultraviolet radiation on morphological and physicochemical properties of sesame protein isolate based edible films. Food Hydrocoll 85:136–143. https://doi.org/10.1016/j.foodhyd.2018.07.018
34. Amjadi S, Almasi H, Pourfathi B, Ranjbaryan S (2021) Gelatin films activated by cinnamon essential oil and reinforced with 1D, 2D and 3D nanomaterials: physical and release controlling properties. J Polym Environ. https://doi.org/10.1007/s10924-021-02097-3
35. Chenwei C, Zhipeng T, Yarui M et al (2018) Physicochemical, microstructural, antioxidant and antimicrobial properties of active packaging films based on poly(vinyl alcohol)/clay nanocomposite incorporated with tea polyphenols. Prog Org Coatings 123:176–184. https://doi.org/10.1016/j.porgcoat.2018.07.001
36. Leite LSF, Ferreira CM, Correa AC et al (2020) Scaled-up production of gelatin-cellulose nanocrystal bionanocomposite films by continuous casting. Carbohydr Polym. https://doi.org/10.1016/j.carbpol.2020.116198
37. George J, Siddaramaiah (2012) High performance edible nanocomposite films containing bacterial cellulose nanocrystals. Carbohydr Polym 87:2031–2037. https://doi.org/10.1016/j.carbpol.2011.10.019
38. Li K, Jin S, Chen H, Li J (2019) Bioinspired interface engineering of gelatin/cellulose nanofibrils nanocomposites with high mechanical performance and antibacterial properties for active packaging. Compos Part B Eng 171:222–234. https://doi.org/10.1016/j.compositesb.2019.04.043
39. Mondragon G, Peodriguez C, Gonzalez A et al (2015) Bionanocomposites based on gelatin matrix and nanocellulose. Eur Polym J 62:1–9
40. Li K, Jin S, Chen H et al (2017) A high-performance Soy protein isolate-based nanocomposite film modified with microcrystalline cellulose and Cu and Zn nanoclusters. Polym (Basel). https://doi.org/10.3390/polym9050167
41. Lima HLS, Gon硬ves C, Cerqueira M et al (2018) Bacterial cellulose nanofiber-based films incorporating gelatin hydrolysate from tilapia skin: production, characterization and cytotoxicity assessment. Cellulose 25:6011–6029. https://doi.org/10.1007/s10570-018-1983-0
42. Fakhreddin Hosseini S, Rezaei M, Zandi M, Ghavi FF (2013) Preparation and functional properties of fish gelatin-chitosan blend edible films. Food Chem 136:1490–1495. https://doi.org/10.1016/j.foodchem.2012.09.081
43. Pelissari FM, Andrade-Mahecha MM, Amaral Sobral PJ, Menegalli FC (2017) Nanocomposites based on banana starch reinforced with cellulose nanofibers isolated from banana peels. J Colloid Interface Sci 505:154–167
44. Shabanpour B, Kazemi M, Ojagh SM, Pourashouri P (2018) Bacterial cellulose nanofibers as reinforce in edible fish myofibrillar protein nanocomposite films. Int J Biol Macromol 117:742–751
45. Hosseini SF, Rezaei M, Zandi M, Farahmandghavi F (2015) Fabrication of bio-nanocomposite films based on fish gelatin reinforced with chitosan nanoparticles. Food Hydrocoll 44:172–182
46. He Q, Zhang Y, Cai X, Wang S (2016) Fabrication of gelatin-TiO2 nanocomposite film and its structural, antibacterial and physical properties. Int J Biol Macromol 84:153–160. https://doi.org/10.1016/j.ijbiomac.2015.12.012
47. Amjadi S, Nazari M, Alizadeh SA, Hamishehkar H (2020) Multifunctional betanin nanoliposomes-incorporated gelatin/chitosan nanofiber/ZnO nanoparticles nanocomposite film for fresh beef preservation. Meat Sci. https://doi.org/10.1016/j.meatsci.2020.108161
48. Azari SS, Alizadeh A, Roufegarinejad L et al (2021) Preparation and characterization of gelatin/β-glucan nanocomposite film incorporated with ZnO nanoparticles as an active food packaging system. J Polym Environ 29:1143–1152
49. Soukoulis C, Behboudi-Jobbehdar S, Yonekura L et al (2014) Stability of *Lactobacillus rhamnosus* GG in prebiotic edible films. Food Chem 159:302–308. https://doi.org/10.1016/j.foodchem.2014.03.008
50. Tibolla H, Pelissari FM, Martins JT et al (2019) Banana starch nanocomposite with cellulose nanofibers isolated from banana peel by enzymatic treatment: in vitro cytotoxicity assessment. Carbohydr Polym 207:169–179. https://doi.org/10.1016/j.carbpol.2018.11.079
51. Almasian A, Najafi F, Eftekhari M et al (2020) Polyurethane/carboxymethylcellulose nanofibers containing *Malva sylvestris* extract for healing diabetic wounds: preparation, characterization, in vitro and in vivo studies. Mater Sci Eng C. https://doi.org/10.1016/j.msec.2020.111039
52. Niu X, Liu Y, Song Y et al (2018) Rosin modified cellulose nanofiber as a reinforcing and co-antimicrobial agents in polylactic acid/chitosan composite film for food packaging. Carbohydr Polym 183:102–109. https://doi.org/10.1016/j.carbpol.2017.11.079
53. Tsai YH, Yang YN, Ho YC et al (2018) Drug release and antioxidant/antibacterial activities of silymarin-zein nanoparticle/bacterial cellulose nanofiber composite films. Carbohydr Polym 180:286–296. https://doi.org/10.1016/j.carbpol.2017.09.100
54. Alizadeh-Sani M, Khezerlou A, Ehsani A (2018) Fabrication and characterization of the bionanocomposite film based on whey protein biopolymer loaded with TiO2 nanoparticles, cellulose

nanofibers and rosemary essential oil. Ind Crops Prod 124:300–315. https://doi.org/10.1016/j.indcrop.2018.08.001
55. Amjadi S, Almasi H, Ghadertaj A, Mehryar L (2020) Whey protein isolate-based films incorporated with nanoemulsions of orange peel (*Citrus sinensis*) essential oil. Prep Charact. https://doi.org/10.1111/jfpp.15196